Sensitivity of the seasonal cycle of CO_2 at remote monitoring stations with respect to seasonal surface exchange fluxes determined with the adjoint of an atmospheric transport model

Thomas Kaminski, Ralf Giering, Martin Heimann
Max Planck Institut für Meteorologie, Bundesstr. 55, D-20146 Hamburg

Camera-ready Copy for
Physics and Chemistry of the Earth
Manuscript-No. OA13.2-08

Offset requests to:
T. Kaminski

Journal: Physics and Chemistry of the Earth
MS No.: OA13.2-08
First author: Kaminski

Sensitivity of the seasonal cycle of CO_2 at remote monitoring stations with respect to seasonal surface exchange fluxes determined with the adjoint of an atmospheric transport model

Thomas Kaminski, Ralf Giering, Martin Heimann
Max Planck Institut für Meteorologie, Bundesstr. 55, D-20146 Hamburg

Received – Accepted – Communicated by

Abstract. The adjoint model to a global three-dimensional atmospheric transport model can be used to efficiently perform a sensitivity analysis, i.e. the computation of the partial derivatives of a particular model output feature with respect to many control variables. We demonstrate this approach by investigating the dependence of the magnitude of the modeled seasonal cycle of CO_2 at remote monitoring stations with respect to the magnitudes of the seasonal cycle of the net CO_2 surface fluxes prescribed from a simple diagnostic terrestrial biosphere model. The technique results in global maps of those source regions that predominately influence the magnitude of the seasonal cycle at the different monitoring stations.

1 Introduction

Observations of the atmospheric CO_2 concentration from the global networks of remote background air monitoring stations provide an indispensable tool to constrain spatial and temporal variations of net surface fluxes of carbon between the atmosphere, the oceans and the terrestrial biosphere (Conway et al., 1994; Keeling et al., 1995). An assessment of this information, however, is complicated by the fact that the three-dimensional atmospheric transport has to be taken into account. During the recent years, a variety of three-dimensional atmospheric transport models have been developed and used to analyse the observations from the monitoring stations (Fung et al., 1983; Heimann et al., 1989; Keeling et al., 1989; Tans et al., 1990; Enting et al., 1995).

Typically, these models are applied for forward simulations, i.e. surface flux fields are prescribed in space and time and the model is used to compute the spatio-temporal variations of the atmospheric CO_2 concentration. However, often the inverse problem is of even greater interest: given observations of the CO_2 concentration at particular monitoring sites, what is the range of possible surface source configurations that are compatible with the data? This problem requires the application of numerical inversion techniques, such as the "synthesis inversion" (Enting et al., 1995) or the adjoint technique (Steinhausen, 1979; Marchuk, 1995).

Here we demonstrate an application of the adjoint model to a three-dimensional transport model as tool for sensitivity analysis. The adjoint model can efficiently compute the partial derivatives of an observational feature (here we take the magnitude of the seasonal cycle of atmospheric CO_2 at a particular station) with respect to a large number of control variables determining surface source features (here we take the magnitude of the net seasonal CO_2 source at each surface grid point of the transport model). These partial derivatives provide a direct visualisation of the surface area that is mapped by atmospheric transport to the chosen observational feature at a particular monitoring station.

In the following we describe briefly the transport model and its adjoint, followed by a formal definition of the chosen observational feature (i.e. the magnitude of the seasonal cycle of CO_2) and the control variables (i.e. the strength of the seasonal surface CO_2 sources). We then apply the adjoint model to eight stations of the NOAA CO_2 monitoring network (Conway et al., 1994) and show in the results section the computed patterns of surface fluxes that influence the particular stations. In the present feasibility study, we limit ourselves to seasonal terrestrial biospheric CO_2 fluxes. Of course, the technique is equally applicable to any other surface flux source.

Correspondence to: T. Kaminski

2 Software

2.1 Atmospheric transport model

TM2 is a three-dimensional atmospheric transport model which solves the continuity equation for an arbitrary number of atmospheric tracers on an Eulerian grid spanning the entire globe (Heimann, 1995). It is driven by stored meteorological fields derived from analyses of a weather forecast model or from output of an atmospheric general circulation model. Tracer advection is calculated using the "slopes scheme" of Russel and Lerner (1981). Vertical transport due to convective clouds is computed using the cloud mass flux scheme of Tiedtke (1989). Turbulent vertical transport is calculated by stability dependent vertical diffusion according to the scheme by Louis (1979). Numerically, in each base time step the model calculates the source and sink processes affecting each tracer, followed by the calculation of the transport processes.

The spatial structure of the model is a regular latitude-longitude grid and a sigma coordinate system in the vertical dimension. The base "coarse grid" version of the model uses a horizontal resolution of approximately 8^o latitude by 10^o longitude (i.e. the horizontal dimension of the grid is $ng = 36 \times 24$) and 9 layers in the vertical dimension. The numerical timestep of this model version is four hours.

In the present study we used the base coarse grid model version with meteorological fields of the year 1987, derived from analyses of the European Center for Medium Range Weather Forecast (ECMWF) which are available to the model every 12 hours. Thereby the meteorological fields have been adjusted in order to guarantee air mass conservation. This adjustment is also applied when switching from the fields of December 31 to January 1 in a multiyear tracer model simulation (Heimann, 1995).

2.2 Tangent linear and Adjoint Model Compiler

As described later in Sect. (3) our approach is based on evaluation of partial derivatives. We need to differentiate a scalar valued function P with respect to a large set of independent "control" variables. In principle, P is not given by an analytical formula, but must be evaluated by execution of a computer programme (here the atmospheric transport model) for a particular vector of control variables. Thus P essentially is defined by a sequence of Fortran 77 (the programming language of the TM2 model) source code statements. Formally, each step of the source code can be seen as an individual differentiable function and P, being the composition of these functions, can be differentiated by use of the chain rule. Thus, the calculation of the partial derivatives results in a multiple product of matrices each corresponding to a particular step in the code. In terms of computational efficiency, for differentiation of scalar valued functions, it is favourable to compute this matrix product in reverse order as compared to the original code. This technique is called "reverse mode" and the code for evaluation of the derivative is called the "adjoint model". The adjoint model can either be constructed by hand or automatically (Giering and Kaminski, 1996). Here, in order to generate the adjoint model of P, we used the newly developed automatic Tangent linear and Adjoint Model Compiler (TAMC, Giering (1996)). This software-tool is a source-to-source translation programme (precompiler) for modules written in Fortran 77 which generates code to evaluate derivatives in forward or reverse mode. In our application, a run of the adjoint model requires about 3–4 times the computation time of a corresponding forward transport model run (i.e. a single evaluation of P).

3 Method

3.1 Simulation of the biospheric component in the seasonal cycle of atmospheric CO_2

In this study, we restrict ourselves to the seasonal cycle of the atmospheric CO_2 concentration generated by the terrestrial biosphere. As a base case we chose the monthly net surface fluxes calculated by the Simple Diagnostic Biosphere Model (SDBM, (Knorr and Heimann, 1995)). This model is based on remote sensing and climate data. Furthermore, the SDBM includes two global tuning parameters that have been determined by minimising the generated atmospheric seasonal cycles at a series of calibrating stations from the NOAA network. The optimised SDBM results in a reasonably accurate representation of the seasonal cycle of the CO_2 concentration at most of the stations of the NOAA network (Knorr and Heimann, 1995; Heimann et al., 1996).

Let f_{ij}^t denote the flux into the TM2 grid cell (i, j) of the first vertical layer in month t. For simulating the seasonal cycle in the concentration TM2 is run for four years by repeatedly cycling through the same meteorological fields of the year 1987 and repeating the seasonal cycle of the SDBM fluxes. After four years, a cyclostationary state in the seasonal cycle of the simulated CO_2 concentration is obtained.

At a particular site S the seasonal cycle in the concentration C_S is computed from the simulated concentration fields of the fourth year with the following procedure: Firstly, monthly means are computed. Secondly, a bilinear interpolation in the horizontal from the TM2 grid to the exact location of S is performed. Finally, the annual mean at S is subtracted. Formally, the seasonal cycle C_S determined by this procedure can be represented as an element of $\mathbb{R}^{12}$, the vector space of real 12-tuples.

3.2 Magnitude of the modeled seasonal cycle

In order to investigate the contributions from the local amplitudes of the CO_2 flux in each grid cell to C_S, the simulated seasonal cycle at station S, we introduce as control variables a vector $X \in \mathbb{R}^{ng}$ consisting of $ng = 36 \times 24$ dimensionless scalar multipliers for the seasonal cycle of the flux in every grid cell.
For each X let $T(X) := C_S$ where C_S is computed as described in Sect. 3.1 from the fluxes $X_{(i,j)} f^t_{ij}$. The base case (i.e. the seasonal cycle generated by the SDBM) is obtained if $X = (1, \ldots, 1)$ which we denote with the subscript 0: $C_{S,0} := T((1, ..., 1))$.
Employing the standard inner product $(\cdot, \cdot)$ of $\mathbb{R}^{12}$ one can define for each X the magnitude of $T(X)$ as a normalised projection of $T(X)$ in the direction of $C_{S,0}$:

$$P(X) \quad := \quad \frac{(T(X), C_{S,0})}{(C_{S,0}, C_{S,0})} \qquad (1)$$

In the base case $P(X_0) = 1$ for $X_0 = (1, ..., 1)$. If $P(X) > 1$ for a particular X, this can be interpreted as an enhanced seasonal cycle as compared to the base case.

3.3 Decomposition of the modeled seasonal cycle

The TAMC is able to generate the code for the simultaneous evaluation of the partial derivatives

$$\frac{\partial P}{\partial X_1}(X), ..., \frac{\partial P}{\partial X_{ng}}(X) \qquad (2)$$

for any vector of control variables X.
Due to the linearity of P the partial derivatives are constant and a Taylor series expansion yields:

$$P(X) - P(X_0) \quad = \quad \sum_{k=1}^{ng} \frac{\partial P}{\partial X_k}(X_k - X_{0,k}) \qquad . \qquad (3)$$

Thus the sensitivity of P to a change in the k-th component of X_0 is $\frac{\partial P}{\partial X_k}$.
Furthermore $\frac{\partial P}{\partial X_k}$ can be interpreted as the portion in the seasonal signal, $C_{S,0}$, that is contributed by the flux from the grid cell (i, j) associated with the index k. This follows from the linearity of P and Eq. (3) by first inserting $X_0 = (1, ..., 1)$ and $X = (1, ..., X_k = 0, ..., 1)$ which yields

$$P((0, ..., X_k = 1, ..., 0)) \quad = \quad \frac{\partial P}{\partial X_k} \qquad (4)$$

and then inserting $X_0 = (1, ..., 1)$ and $X = (0, ..., 0)$ which yields

$$1 = P((1, ..., 1)) \quad = \quad \sum_{k=1}^{ng} \frac{\partial P}{\partial X_k} \qquad . \qquad (5)$$

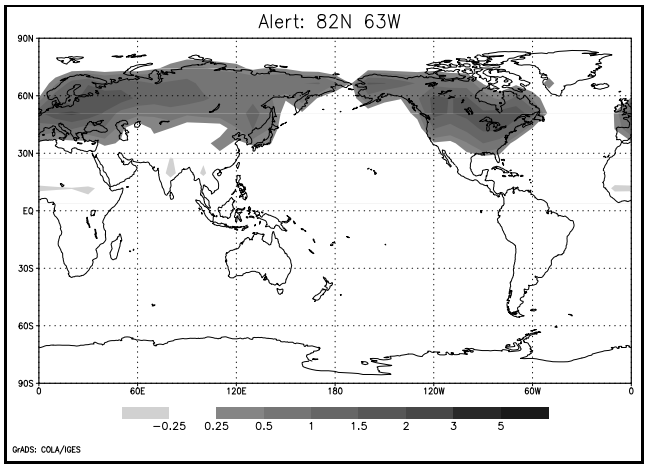

Fig. 1. Contribution to the magnitude of the seasonal cycle at Alert in per cent

4 Results

Using the adjoint model code we have computed the partial derivatives $\frac{\partial P}{\partial X_k}$, $(k = 1, \ldots, ng)$, for eight different stations of the NOAA network. Figs. 1–8 show the resulting maps of the partial derivatives for each of the stations. These maps may be interpreted as the areas that contribute to the seasonal cycle as "seen" by the particular station. The displayed numbers are scaled such that the sum over all gridpoints equals 100%. Negative values correspond to regions in which the magnitude of the seasonal source must be reduced in order to enhance the seasonal cycle at the target station.
The two arctic stations Alert (82N, 62W, Fig. 1) and Point Barrow (71N, 156W, Fig. 2) exhibit relatively similar spatial patterns: both record primarily the northern hemisphere temperate latitude terrestrial biosphere regions. Point Barrow, lying closer to gridpoints with substantial seasonal terrestrial fluxes, shows a slightly more enhanced contribution from the Alaskan peninsula.
The station Cape Meares (45N, 124W, Fig. 4) is heavily dominated by contributions from the western part of the North American continent, whereas Shemya Island (53N, 174W, Fig. 3) sees a substantial contribution from the easternmost parts of the Asian continent.
As expected, the background station Mauna Loa on Hawaii (19N, 155W, Fig. 5) monitors essentially the entire northern hemisphere. In addition, the patterns also reveal a substantial contribution from the Tropics (Amazon region, central Africa). Furthermore, the seasonal CO_2 exchanges in the monsoon dominated regime of India and to some extent of southeastern Asia influence the seasonal cycle at Mauna Loa in a negative sense.
The terrestrial biosphere seasonal cycle of CO_2 at the station Ascencion Island (8S, 14W, Fig. 6) in the Atlantic Ocean is dominated by the seasonal exchanges in

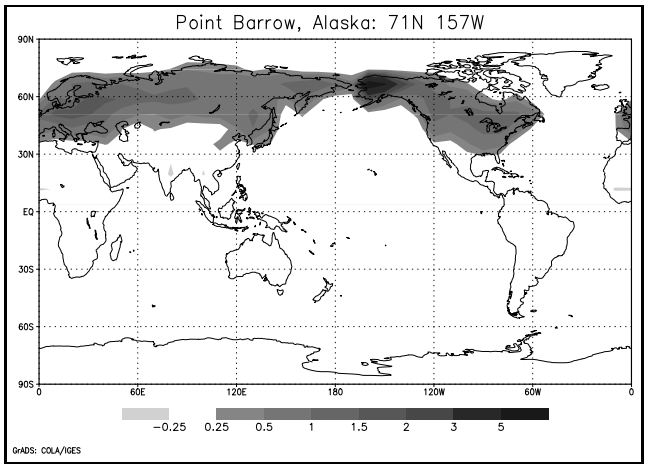

Fig. 2. Contribution to the magnitude of the seasonal cycle at Point Barrow in per cent

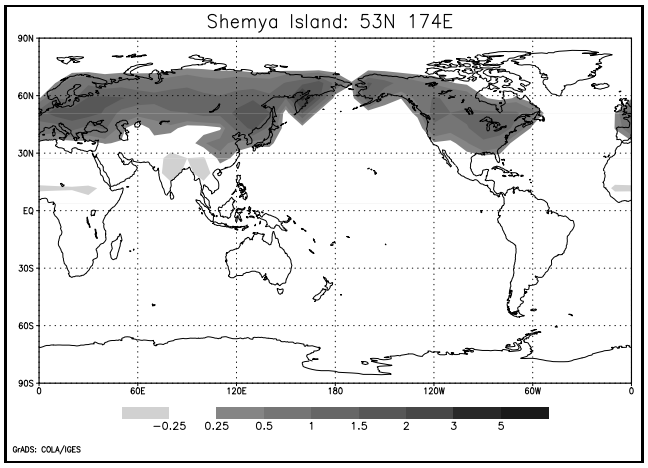

Fig. 3. Contribution to the magnitude of the seasonal cycle at Shemya Island in per cent

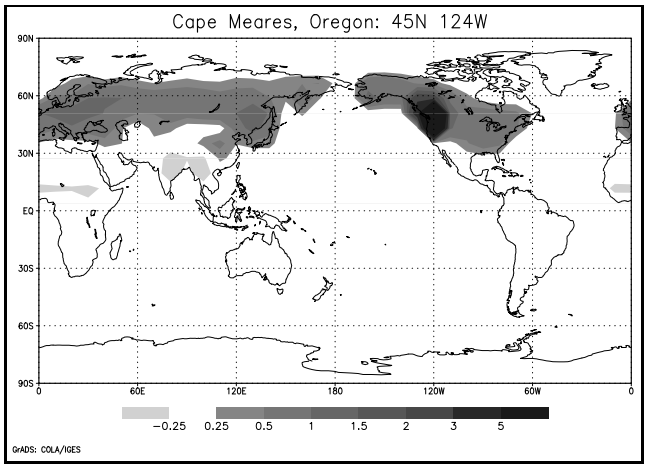

Fig. 4. Contribution to the magnitude of the seasonal cycle at Cape Meares in per cent

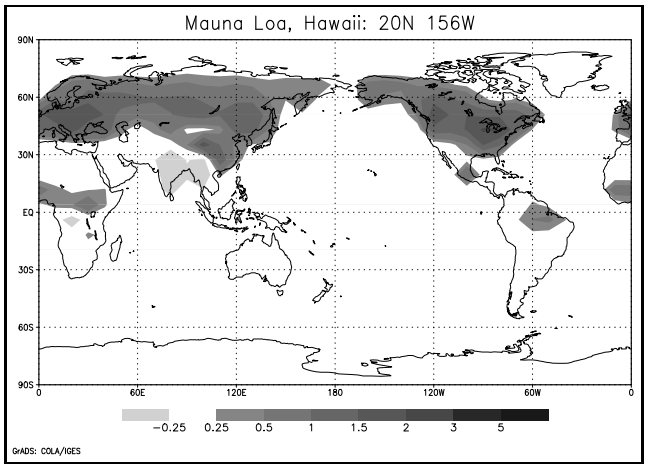

Fig. 5. Contribution to the magnitude of the seasonal cycle at Mauna Loa in per cent

southequatorial Africa and southern South America to about the same extent. The map of partial derivatives also reveals that both the northern hemisphere temperate latitudes and southern Australia and New Zealand also contribute to the signal at this site. Conversely, the Cape Grim station (41S, 145E, Fig. 7) is heavily dominated by seasonal exchanges in nearby Australia and, to some minor extent from the tropical regions.

Finally, the South Pole station (Fig. 8) shows a relatively complex pattern, with about equal contributions from the temperate latitude biosphere in each hemisphere and the tropics. However, there are also several regions (India, southequatorial Africa, northern Australia and parts of Brazil south of the Amazon region) where the seasonal terrestrial source excerts a negative influence on the CO_2 cycle at the South Pole.

The differences between the maps from Cape Grim and the South Pole are quite striking considering the fact that both stations represent southern hemisphere "background monitoring" stations. It must be noted, though, that we did not perform a detailed selection procedure according to air-mass origin in calculating the modelled monthly mean CO_2 concentration at Cape Grim. Such a procedure seems necessary in order to correctly compare model and observations at this site (Ramonet and Monfray, 1996). If a selection procedure were performed in the model, then the computed influence pattern for the seasonal cycle at Cape Grim most probably would look similar to the South Pole station pattern.

5 Discussion

The present study demonstrates a technique of analysing the modeled seasonal cycle of CO_2 in terms of a composition of contributions originating from the respective local seasonal CO_2 fluxes from the biosphere to the atmosphere. Clearly, the computed patterns of local contributions are not model independent, but through our choice of measure for the magnitude of the seasonal cycle (Eq. (1)) depend on the base case $C_{S,0}$, i.e. the

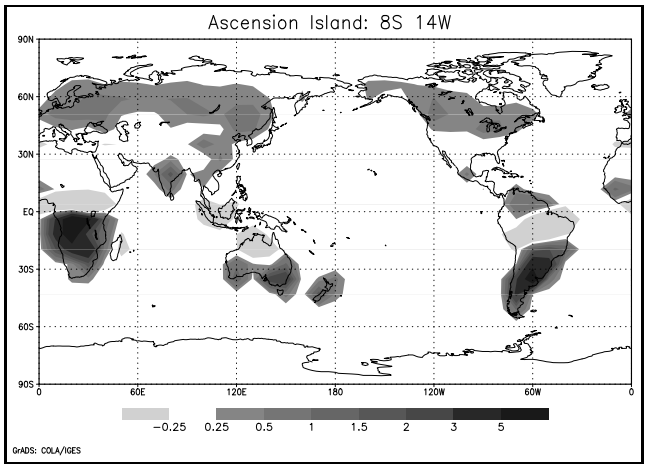

Fig. 6. Contribution to the magnitude of the seasonal cycle at Ascencion Island in per cent

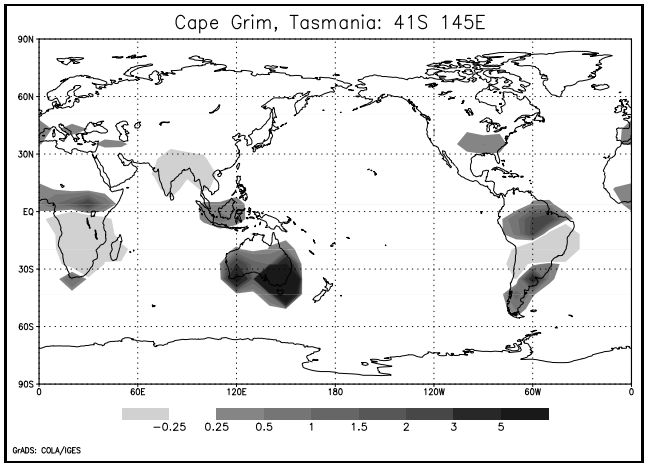

Fig. 7. Contribution to the magnitude of the seasonal cycle at Cape Grim in per cent

fluxes from the SDBM model. Nevertheless, most of the features seen in Figs. 1–8 reflect properties of the transport from the different terrestrial biospheric source regions to the monitoring station under consideration and would not be altered substantially by using a different set of terrestrial seasonal CO_2 fluxes.

By the same technique we also studied the sensitivity of the magnitude of the seasonal cycle with respect to a change in the local phase of the seasonal surface fluxes rather than their amplitude. The analysis results in similar patterns for the eight stations as shown here.

Each of the eight influence patterns was computed by a single run of the adjoint model with a computational cost corresponding to the cost of 3–4 forward model runs. Alternatively, the same result could have been obtained by performing $ng = 36 \times 24$ forward model runs (or a single forward model run with ng tracers), each with the prescribed seasonal cycle of surface fluxes at a particular gridcell. Thus, as long as the number of components (ng) is larger than the number of stations

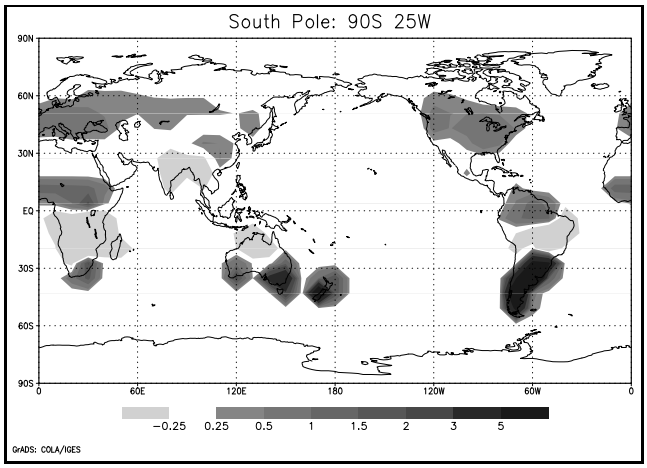

Fig. 8. Contribution to the magnitude of the seasonal cycle at the South Pole in per cent

by a factor of 3-4, the adjoint approach is computationally more efficient.

The present approach promises several extensions. The spatial resolution can be improved by use of a higher resolution transport model. Clearly, the technique can also be applied to decompose the contributions of different source regions of oceanic and fossil fuel CO_2.

Acknowledgements. The authors thank Wolfgang Knorr for providing the SDBM fluxfields. This work was supported in part by the Commission of the European Communities under contracts ENV4-CT95-0116 and EV5V-CT92-0120, European Study of Carbon in the Oceans Biosphere and Atmosphere (ESCOBA): Atmosphere Section. Computing support was provided by the Deutsches Klimarechenzentrum (DKRZ) in Hamburg.

References

Conway, T. J., Tans, P., Waterman, L., Thoning, K., Buanerkitzis, D., Masarie, K., and Zhang, N., Evidence for interannual variability of the carbon cycle from the noaa–cmdl global air sampling network, *J. Geophys. Res., 99D*, 831–855, 1994.

Enting, I. G., Trudinger, C. M., and Francey, R. J., A synthesis inversion of the concentration and $\delta^{13}C$ of atmospheric CO_2., *Tellus*, (47B), 35–52, 1995.

Fung, I., Prentice, K., Matthews, E., Lerner, J., and Russel, G., Three-dimensional tracer model study of atmospheric CO_2 : response to seasonal exchanges with the terrestrial biosphere, *J.Geophys.Res.*, (88), 1281–1294, 1983.

Giering, R., *Tangent linear and Adjoint Model Compiler, users manual*, MPI, Bundesstr. 55, 20251 Hamburg, Germany, 1996.

Giering, R. and Kaminski, T., Recipes for Adjoint Code Construction, *Submitted to ACM Transactions on Mathematical Software*, 1996.

Heimann, M., The global atmospheric tracer model TM2, Technical report no. 10, Max-Planck-Institut für Meteorologie, Bundesstr. 55, 20251 Hamburg, Germany, 1995.

Heimann, M., Keeling, C. D., and Tucker, D. J., A three-dimensional model of the atmospheric CO_2-transport based on observed winds, in *Aspects of climate Variability*, edited by D. H. Peterson, chap. 2. Model description and simulated tracer experiments, 1989.

Heimann, M., Esser, G., Haxeltine, A., Kaduk, J., Kicklighter, D. W., Knorr, W., Kohlmaier, G. H., McGuire, A. D., Melillo, J., Moore, B., Otto, R. D., Prentice, I. C., Sauf, W., Schloss, A., Sitch, S., Wittenberg, U., and Würth, G., Evaluation of terrestrial carbon cycle models through simulations of the seasonal cycle of atmospheric CO_2: First results of a model intercomparison study, *Submitted to Global Biogeochemical Cycles*, 1996.

Keeling, C. D., Piper, S. C., and Heimann, M., A three-dimensional model of the atmospheric CO_2-transport based on observed winds, in *Aspects of climate Variability*, edited by D. H. Peterson, chap. 2. Mean annual gradients and interannual variations, 1989.

Keeling, C. D., Whorf, T. P., Wahlen, M., and van der Plicht, J., Interannual extremes in the rate of rise of atmospheric carbon dioxide since 1980, *Nature*, (375), 666–670, 1995.

Knorr, W. and Heimann, M., Impact of drought stress and other factors on seasonal land biosphere CO_2 exchange studied through an atmospheric tracer transport model, *Tellus*, (47B), 471–489, 1995.

Louis, J. F., A parametric model of vertical eddy fluxes in the atmosphere, *Boundary Layer Meteorology*, (17), 187–202, 1979.

Marchuk, G. I., *Adjoint Equations and Analysis of Complex systems*, Kluwer Academic Publishers, Dordrecht, The Netherlands, 1995.

Ramonet, M. and Monfray, P., CO_2 baseline concept in 3-d atmospheric transport models, *Tellus, in press*, 1996.

Russel, G. L. and Lerner, J. A., A new finite-differencing scheme for the tracer transport equation, *J. Appl. Met.*, pp. 1483–1498, 1981.

Steinhausen, S. W., On studies of the tropospheric temperature field formation with the aid of the conjugate equation method, *Meteorologiya y Gidrologiya*, (3), 37–42, 1979.

Tans, P. P., Fung, I. Y., and Takahashi, T., Observational constraints on the global atmospheric CO_2 budged, *Science*, (247), 1431–1438, 1990.

Tiedtke, M., A comprehensive mass flux scheme for cumulus parameterization in large-scale models, *Mon. Weath. Rev*, (117), 1779–1800, 1989.